PROCEEDINGS OF SPIE

SPIEDigitalLibrary.org/conference-proceedings-of-spie

Effect of matrix anisotropy on the apparent emitter orientation in Organic LED

Norbert Danz, Nils Haase, Antonia Morherr, Christof Pflumm, Birk Fritsch, et al.

Norbert Danz, Nils Haase, Antonia Morherr, Christof Pflumm, Birk Fritsch, Dirk Michaelis, "Effect of matrix anisotropy on the apparent emitter orientation in Organic LED," Proc. SPIE 10687, Organic Electronics and Photonics: Fundamentals and Devices, 106870U (22 May 2018); doi: 10.1117/12.2306408

SPIE.

Event: SPIE Photonics Europe, 2018, Strasbourg, France

Effect of matrix anisotropy on the apparent emitter orientation in Organic LED

Norbert Danz*[a], Nils Haase[b], Antonia Morherr[b], Christof Pflumm[b], Birk Fritsch[a], Dirk Michaelis[a]

[a] Fraunhofer Institute for Applied Optics and Precision Engineering IOF, Albert-Einstein-Str. 7, 07745 Jena, Germany;
[b] Merck KGaA, OLED Physics & Applications, Frankfurter Str. 250, 64293 Darmstadt, Germany

ABSTRACT

Spontaneously aligning emitter molecules can improve the external efficiency of OLED devices and have been reported for different types of emitters doped into suitable hosts. Similar to the morphological alignment of the active molecules, a birefringence of the host affects the apparent emitter orientation. In order to investigate this effect experimentally, $Ir(ppy)_3$ is co-evaporated into the emitting layer of OLED using hosts with different birefringence properties. Analyzing the electroluminescence emission patterns quantitatively reveals the apparent orientation distribution of the emitters. The results emphasize that host birefringence can be used to suppress perpendicular emitter contributions while amplifying the impact of the horizontal dipoles, thus leading to an enhanced forward emission.

Keywords: organic light-emitting diode, electroluminescence, birefringence, emitter orientation, optical simulation

1. INTRODUCTION

Organic Light-Emitting Diodes (OLED) have conquered display applications and remain a candidate for large area solid state lighting applications. Although enormous progress achieved concerning device efficiency and lifetime, the out-coupling of light generated inside the high refractive index organic layers remains a challenging topic for further performance increase of the technology. One promising approach is to exploit aligned emitter molecules in order to support direct emission into the far-field and to reduce optical losses [1, 2]. Following initial observations for fluorophores [3] and phosphors [4], spontaneous alignment of the transition dipole moments can be observed for TADF emitters as well [5], resulting in numerous emitting species [6] that might yield devices with orientation enhanced brightness and efficiency.

The phenomenological orientation of the emitting molecular ensemble is accessed experimentally by emission pattern analyses [7, 8] with subsequent reverse simulation. Such approach requires the precise knowledge of the stack geometry as well as that of the material properties. Advanced approaches suggested a very good alignment of the emitting ensembles recently [9, 10]. Regarding emitter orientation, especially the anisotropic properties of both the thin film system as well as that of the emitting layer (EML) need to be considered. Birefringence of the ETL or HTL layers modifies the propagation of light fields in the cavity and can be used to optimize out-coupling [11]. Birefringence of the emitting layer has been investigated as well [12, 13,] but without cross checking different anisotropic (host) materials experimentally.

The following approach is conducted in order to access the effect of the EML birefringence on the apparent emitter orientation systematically. Primary emitter orientation can be excluded as much as possible by choosing $Ir(ppy)_3$ as emitting molecule, which is believed to exhibit an isotropic orientation of the dipole transition moments intrinsically [14]. This emitter is doped into three different matrix materials featuring positive, negative, and near zero birefringence when comparing the ordinary and extraordinary refractive indices of a uniaxial model. In result, the effect of host anisotropy onto the apparent emitter orientation is measured by analyzing the far-field emission patterns of adapted OLED devices.

*norbert.danz@iof.fraunhofer.de; phone +49 3641 807750

Organic Electronics and Photonics: Fundamentals and Devices, edited by Sebastian Reineke, Koen Vandewal, Proc. of SPIE Vol. 10687, 106870U · © 2018 SPIE
CCC code: 0277-786X/18/$18 · doi: 10.1117/12.2306408

2. EXPERIMENTAL APPROACH

2.1 OLED Preparation

All experiments have been performed using bottom emitting OLED stacks. Figure 1(a) illustrates the OLED thin film stack as well as the key parameters of the system. This stack utilizes commercial ITO coated substrates, which have been coated after an initial cleaning procedure with the hole injection layer (HIL), hole transport layer (HTL), emissive layer (EML), electron transport layer (ETL) and a metal cathode (LiQ with Aluminum). The emissive area of the OLED devices was limited to 2 x 2 mm^2 by using proper shadow masks during deposition.

Three different OLED stacks have been prepared in order to allow for an emission pattern based measurement of the emitter orientation according to [7, 15]. These OLED differ in the choice of the EML's host material only, which contained a 5% $Ir(ppy)_3$ concentration in all cases. Figure 1(b, c) plot the dispersion of these hosts featuring qualitatively different birefringence properties.

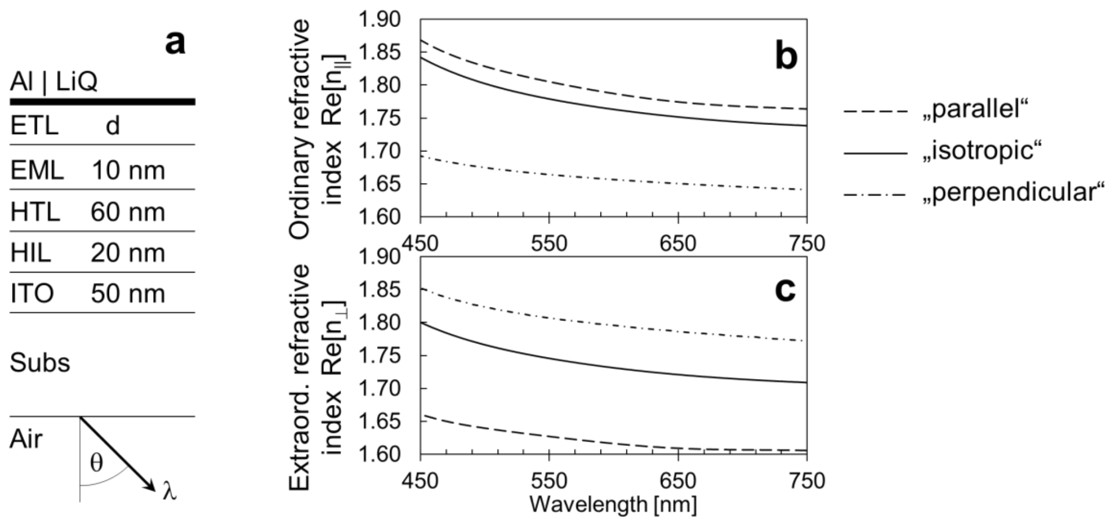

Figure 1. Sketch of the OLED thin film stack (a, thicknesses not scaled), for which the ETL thickness d has been adapted for emission zone and orientation analysis. The diagrams illustrate the dispersion of the refractive index real (b) and imaginary (c) parts of the three host materials, which are referred to as parallel, isotropic, and perpendicular hosts.

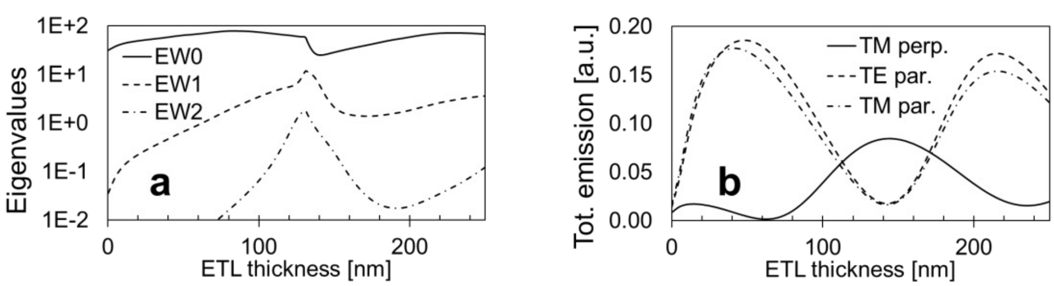

Figure 2. Design of the correct ETL for emission pattern analysis. (a) The highest three eigenvalues for emission zone analysis based on TE polarized pattern in air [16]. (b) Total emitted energy of strictly parallel or strictly perpendicular emitters into the far field in air.

Additional deposition runs have been performed to access tooling factors and layer thicknesses, where the ETL's thickness is the most important parameter for accurate optical reverse simulations. The design thickness of the ETL needs to be optimized for ideal emission zone estimation of the TE polarized pattern [16] as well as for optimum visibility of perpendicular emitters in TM polarization [15]. Both considerations are plotted in Figure 2 and yield an optimum ETL thickness for emission zone analysis of 134 nm (Figure 2a), while the best visibility of perpendicular emitters is predicted in the 140…145 nm range (Figure 2b).

2.2 Emission Pattern Measurement

The emission patterns have been measured using a constant current source (Yokogawa) at a current density of 5 mA/cm^2. OLEDs mounted on a goniometer stage (Thorlabs) have been rotated in steps of 3°. The collection of emission spectra utilized wire grid linear polarizer combined with a quarter-wave plate in order to couples circularly polarized light into a multimode step index fiber (Thorlabs). Spectral emission has been recorded by a fiber spectrometer (Ocean Optics) and 2 nm spectral step width.

Besides the measurement of far-field emission patterns in air, the emission pattern inside the OLED substrate glass has been accessed as well. Therefore, a thinned half ball lens made of B270 was immersion coupled to the OLED. The dispersion properties of B270 have been assumed in the far-field simulation.

All patterns have been recorded in the full angular range -90°…+90° to cross check the symmetry of the spectra. Prior to analysis, all spectra were background corrected and spectra pairs taken at positive and negative angles have been averaged.

2.3 Simulation and Data Analysis

The simulation relies on the dyadic Green's function approach [17] implemented for OLED modelling in the tool RadiatingSlabs as reported previously [4, 7, 9, 15, 16, 18]. This numerical model includes arbitrary orientation distributions, Purcell effect consideration as well as multiple incoherent reflexes in the substrates of large area sources. Birefringence of not-emitting layers [11] is considered by applying appropriate transition conditions for the electromagnetic field at the interfaces between neighboring thin films. Materials used in the stack have been analyzed by means of model-free dispersion analysis [19] to extract the ordinary dispersion ($n_{\|}+ik_{\|}$). Furthermore, anisotropic dispersion ($n_{\perp}+ik_{\perp}$) is obtained by additional ellipsometric investigations [20].

Concerning the birefringence of the EML, several electrodynamic models have been proposed [12, 13]. The EML birefringence influences interference phenomena inside the cavity as well as the density of relevant modal states. Because of the rather small EML thickness, the interference properties and the modal density are modified by birefringence marginally only. Additionally, birefringence affects parallel and perpendicular dipole moments differently. Such effect can be included in the emitter's dipole strength and thus be interpreted as an altered emitter orientation. Therefore, we consider the EML to exhibit isotropic dispersion properties and any anisotropy present in the EML is interpreted to arise due to emitter orientation. This allows us to compare the impact of different birefringent host materials onto the apparent emitter orientation, and to quantitatively compare the effect with reported results on emitter alignment.

In a first step, the TE-polarized emission patterns are analyzed to extract the emission zone of the device [16], thereby deriving the intrinsic spectrum as well [21]. Subsequently, the ensemble orientation is derived from the TM polarized emission pattern while assuming the emission zone and intrinsic spectrum as obtained from the first step. Note that this approach involves the full emission patterns and does not rely on monochrome measurements only. Below, the ratio $|p_{\|}|^2:|p_{\perp}|^2$ of parallel vs. perpendicular emitter contribution determines the (average) orientation of the emitter ensemble, which becomes $|p_{\|}|^2:|p_{\perp}|^2=2:1$ in the isotropic case. Alternatively, the value

$$a_{\perp}=\frac{|p_{\perp}|^2}{|p_{\perp}|^2+|p_{\|}|^2}$$

describing the perpendicular emitter contribution will be used. This value becomes $a_{\perp}=1/3$ for isotropic distributions.

3. RESULTS AND DISCUSSION

Figure 3 illustrates the emission patterns obtained for the three different OLED stacks with and without using an immersion coupled half ball lens. The far-field patterns in air shown in the upper row represent the patterns used for fitting the emission zone from the TE polarized data as well as the orientation of the emitter ensemble from the TM polarized data. Despite the fact that birefringence is ignored in the simulation, i.e., that the ordinary refractive index ($n_{\|}$) is considered for the EML only, the patterns are described almost perfectly for both polarizations and for all hosts. This very good coincidence of simulation and experiment was expected because of the minor influence of the EML birefringence on the light interference properties resulting from the very small EML thickness. Therefore, the OLED emission patterns allow to derive results for the apparent ensemble orientation that is shown in Figure 4. Such approach corresponds to modelling all orientation anisotropy solely by the emitter orientation while neglecting orientation effects of the host.

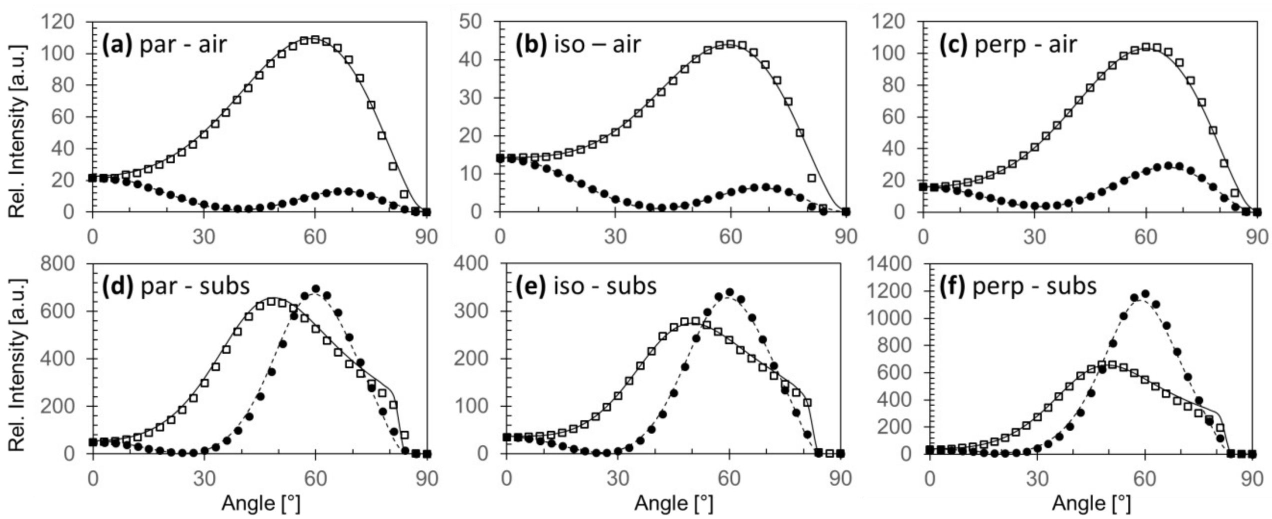

Figure 3: Monochrome emission patterns obtained in air (a-c) or in substrate by means of an immersion coupled half ball lens (d-f) for the “parallel” host (a, d), the “isotropic” host (b, e), and the “perpendicular” host (c, f). All diagrams plot TE measurements (full circles) with TE simulation (dashed) as well as TM measurements (empty squares) with TM simulation (straight line).

The EML model obtained from fitting the air patterns has been used to cross check its applicability to substrate patterns. There, erroneous material birefringence could become apparent in the TM polarized emission at large angles. Interestingly, the results do not reveal such effect, because the pattern of all three OLED could be described well by assuming isotropic EML with oriented emitters. The fact that emission is zero for large angles exceeding 82° is due to a slightly higher refractive index of the half ball lens compared to the OLED substrate. But such effect is readily considered in the simulations.

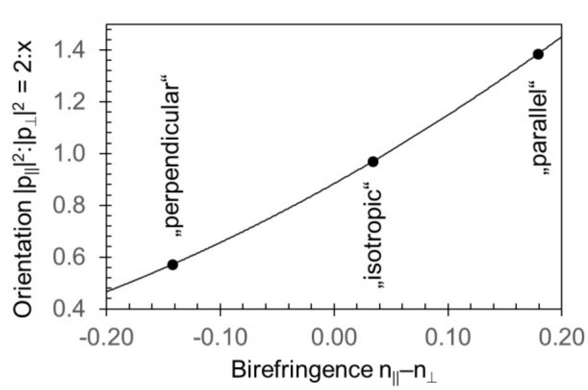

Figure 4: Apparent emitter orientation $|p_{\|}|^2:|p_\perp|^2=2:|p_\perp|^2$ vs. host anisotropy determined from OLED emission pattern measurement and subsequent reverse simulation. The dots plot the experimental results and approximately indicate the error interval that is in the range $\Delta(|p_\perp|^2) \sim \pm 0.03$. The line is a guide for the eye only.

The orientation result in Figure 4 reveals a huge effect of the host anisotropy onto the apparent emitter orientation. For the “isotropic” host the orientation $|p_{\|}|^2:|p_\perp|^2=2:0.97$ ($a_\perp=0.33$) of an almost perfect isotropic ensemble is found. The birefringence of the host modifies this observation considerably. While the EML with increased ordinary refractive index increases the contribution of perpendicular emitters to 2:1.39 ($a_\perp$=0.41), the host with increased extraordinary index perpendicular host yields a preferred parallel orientation of 2:0.57 ($a_\perp$=0.22).

Several results on the orientation of $Ir(ppy)_3$ have been reported recently. These include OLED emission pattern [18, 22, 23], photoluminescence [1, 6, 24, 25], and decay based [26] data. The authors do not explicitly describe the handling of birefringence, especially that of the EML, usually. However, the present result needs to be compared with the outcome of these works, most of which reporting an ideal isotropic orientation of the transition dipole moments of $|p_\parallel|^2:|p_\perp|^2=2:1$ or the corresponding result of $a_\perp$=0.333 [1, 6, 18, 24, 25]. Whilst also preferred parallel orientation of $a_\perp$=0.28 has been measured [26], many works observe a slightly preferred parallel orientation in the range around $|p_\parallel|^2:|p_\perp|^2\sim 2:0.9$ or $a_\perp\sim 0.31$ [22, 23, 25].

4. SUMMARY AND CONCLUSIONS

We have used $Ir(ppy)_3$ as electroluminescent molecule, which is believed to be oriented isotropically in order to verify the effect of host birefringence experimentally. Three different matrix materials featuring positive, negative, and near zero birefringence have been utilized for creating the emitting layer. This allows us to analyze the effect of birefringence onto the apparent emitter orientation. The latter has been extracted from the electroluminescent far-field emission of adapted OLED stacks. Analyzing the data with an isotropic dispersion model for the EML yields the following results:

First, the emission patterns can be fitted well without assuming EML birefringence. This applies to substrate patterns, too, because the very thin EML has minor effect onto the interference properties of the total OLED stack. Additionally, this observation illustrates for a typical OLED configuration that EML birefringence and orientation effects can be confused easily when not analyzing the birefringence properties of the materials well. Second, the analysis yields different orientation results depending on the host used. We obtain a perpendicular emitter contribution to the emission pattern in the range of $a_\perp$=22%…41% (with 33% corresponding to isotropy). The isotropic host yields the expected isotropic emitter orientation. The host with increased perpendicular refractive index ($n_\perp > n_\parallel$) suppresses the emission of perpendicular dipoles, thus exhibiting a strongly preferred parallel, apparent emitter orientation. The contrary effect is found for the case of a host with reduced extraordinary index ($n_\perp < n_\parallel$).

It is worth to note that the “best” orientation derived for $Ir(ppy)_3$ of $|p_\parallel|^2:|p_\perp|^2=2:0.57$ in the “perpendicular” host outperforms the one of $Ir(MDQ)_2acac$ [4], which was the first phosphor reported to align spontaneously. So adjusting the birefringence of the host may optically suppress perpendicular emitter contributions while amplifying the impact of the horizontal dipoles, thus leading to an enhanced forward emission.

ACKNOWLEDGMENT

The authors acknowledge funding by the European Commission under grant no. 732013 (“HyperOLED”).

REFERENCES

[1] Brütting, W., Frischeisen, J., Schmidt, T. D., Scholz, B. J. and Mayr, C., “Device efficiency of organic light-emitting diodes: Progress by improved light outcoupling,” Phys. Status Solidi A 210, 44–65 (2013).
[2] Gather, M. C. and Reineke, S., “Recent advances in light outcoupling from white organic light-emitting diodes,” J. Photon. Energy 5, 057607 (2015).
[3] Yokoyama, D., Sakaguchi, A., Suzuki, M. and Adachi, C., “Horizontal orientation of linear-shaped organic molecules having bulky substituents in neat and doped vacuum-deposited amorphous films,” Org. Electron. 10, 127–137 (2009).
[4] Flämmich, M., Frischeisen, J., Setz, D. S., Michaelis, D., Krummacher, B. C., Schmidt, T. D., Brütting, W. and Danz, N., “Oriented phosphorescent emitters boost OLED efficiency,” Organic Electronics 12, 1663–1668 (2011).
[5] Mayr, C., Lee, S. Y., Schmidt, T. D., Yasuda, T., Adachi, C. and Brütting, W., “Efficiency enhancement of organic light-emitting diodes incorporating a highly oriented thermally activated delayed fluorescence emitter,” Adv. Func. Mat. 24, 5232–5239 (2014).

[6] Schmidt, T. D., Lampe, T., Sylvinson M. R., D., Djurovich, P. I., Thompson, M. E. and Brütting, W., "Emitter orientation as a key parameter in organic light-emitting diodes," Phys. Rev. Appl. 8, 037001 (2017).
[7] Flämmich, M., Gather, M. C., Danz, N., Michaelis, D., Bräuer, A. H., Meerholz, K. and Tünnermann, A., "Orientation of emissive dipoles in OLEDs: Quantitative in situ analysis," Org. Electron. 11, 1039-1046 (2010).
[8] Frischeisen, J., Yokoyama, D., Adachi, C. and Brütting, W., "Determination of molecular dipole orientation in doped fluorescent organic thin films by photoluminescence measurements," Appl. Phys. Lett. 96, 073302 (2010).
[9] Mac Ciarnain, R., Michaelis, D., Wehlus, T., Rausch, A. F., Wehrmeister, S., Schmidt, T. D., Brütting, W., Danz, N., Bräuer, A. and Tünnermann, A., "Plasmonic Purcell effect reveals obliquely ordered phosphorescent emitters in Organic LEDs," Sci. Reports 7, 1826 (2017).
[10] Murawski, C., Elschner, C., Lenk, S., Reineke, S. and Gather, M. C., "Investigating the molecular orientation of Ir(ppy)3 and Ir(ppy)2(acac) emitter complexes by X-ray diffraction," Org. Electron. 53, 198-204 (2018).
[11] Callens, M. K., Yokoyama, D. and Neyts, K., "Anisotropic materials in OLEDs for high outcoupling efficiency," Opt. Express 23, 21128-21148 (2015).
[12] Penninck, L., De Visschere, P., Beeckman, J. and Neyts, K., "Dipole radiation within one-dimensional anisotropic microcavities: a simulation method," Optics Express 19, 18558-18576 (2011).
[13] Moon, C.-K., Kim, S.-Y., Lee, J.-H. and Kim, J.-J., "Luminescence from oriented emitting dipoles in a birefringent medium," Opt. Express 23, A279-A291 (2015).
[14] Steiner, F., Bange, S., Vogelsang, J. and Lupton, J. M., "Spontaneous fluctuations of transition dipole moment orientation in OLED triplet emitters," J. Phys. Chem. Lett. 6, 999−1004 (2015).
[15] Flämmich, M., Michaelis, D. and Danz, N., "Accessing OLED emitter properties by radiation pattern analyses," Org. Electron. 12, 83-91 (2011).
[16] Danz, N., Flämmich, M., Setz, D. S., Krummacher, B. C., Michaelis, D. and Dobbertin, T., "Detection of sub-10 nm emission profile features in organic light-emitting diodes using destructive interference," Opt. Lett. 37, 4134-4136 (2012).
[17] Danz, N., Heber, J., Bräuer, A. and Kowarschik, R., "Dipole lifetime in stratified media," JOSA B 19(3), 412-419 (2002).
[18] Setz, D. S., Schmidt, T. D., Flämmich, M., Nowy, S., Frischeisen, J., Krummacher, B. C., Dobbertin, T., Heuser, K., Michaelis, D., Danz, N., Brütting, W. and Winnacker, A., "Comprehensive efficiency analysis of organic light-emitting devices," J. Photon. Energy 1, 01106 (2011).
[19] Flämmich, M., Danz, N., Michaelis, D., Bräuer, A., Gather, M. C., Kremer, J. H.-W. M. and Meerholz, K., "Dispersion-model-free determination of optical constants: application to materials for organic thin film devices," Applied Optics 48, 1507-1513 (2009).
[20] Tompkins, H. G. and Irene, E. A., [Handbook of ellipsometry], William Andrew and Springer, (2005).
[21] van Mensfoort, S. L. M., Carvelli, M., Megens, M., Wehenkel, D., Bartyzel, M., Greiner, H., Janssen, R. A. J., and Coehoorn, R., "Measuring the light emission profile in organic light-emitting diodes with nanometre spatial resolution," Nature Photon. 4, 329-335 (2010).
[22] Liehm, P., Murawski, C., Furno, M., Lüssem, B., Leo, K. and Gather, M. C., "Comparing the emissive dipole orientation of two similar phosphorescent green emitter molecules in highly efficient organic light-emitting diodes," Appl. Phys. Lett. 101, 253304 (2012).
[23] Graf, A., Liehm, P., Murawski, C., Hofmann, S., Leo, K. and Gather, M. C., "Correlating the transition dipole moment orientation of phosphorescent emitter molecules in OLEDs with basic material properties," J. Mater. Chem. C 2, 10298–10304 (2014).
[24] Kim, K.-H., Moon, C.-K., Lee, J.-H., Kim, S.-Y. and Kim, J.-J., "Highly efficient organic light-emitting diodes with phosphorescent emitters having high quantum yield and horizontal orientation of transition dipole moments," Adv. Mater. 26, 3844–3847 (2014).
[25] Lampe, T., Schmidt, T. D., Jurow, M. J., Djurowich, P. I., Thompson, M. E. and Brütting, W., "Dependence of phosphorescent emitter orientation on deposition technique in doped organic films," Chem. Mater. 28, 712-715 (2016).
[26] Penninck, L., Steinbacher, F., Krause, R. and Neyts, K., "Determining emissive dipole orientation in organic light emitting devices by decay time measurement," Org. Electron. 13, 3079–3084 (2012).